

# Particle velocity, electron temperature, and density profiles of pulsed laser-induced plasmas in air at different ambient pressures

B.Y. Man

Department of Physics, Shandong Normal University, Jinan, 250014, P.R. China  
(Fax: +86-001/0531-6956-954, E-mail: byman@public.jn.sd.cn)

Received: 18 August 1997/Revised version: 9 March 1998

**Abstract.** A time- and space-resolved diagnostic technique was used to study the emission spectra from the plasmas produced by 1.06- $\mu\text{m}$ , 10-ns pulsed-laser irradiation of titanium alloy targets in air at different ambient pressures in the wavelength range of 200 nm to 800 nm. From the time-of-flight (TOF) curves of specific spectrum lines of excited Ti and Fe atoms, the velocities of excited neutral Ti and Fe atoms at different ambient pressures were measured. Under the assumption of local thermodynamic equilibrium (LTE), the electron temperature and the electron number density were deduced from, respectively, the relative line intensity and the Stark-broadening measurements conducted at different ambient pressures. Finally, the validity of application of LTE was discussed.

**PACS:** 79.20.D; 52.50Jm

Pulsed laser ablation of solid materials is becoming more and more important for elemental analysis of a wide variety of solid samples and many other applications. One of the typical applications is pulsed laser deposition (PLD) technique for preparing thin film materials such as high-temperature superconductors [1–3]. The quality of the prepared film using the technique is closely related to the properties of pulsed laser-induced plasmas such as the particle velocity, the temperature, and the number density distribution of the particles in the plasmas. The properties of a plasma can be influenced to a great extent by the ambient pressure [4–7]. In the present work, the optical emission from the plasma produced by a 1.06- $\mu\text{m}$ , 10-ns YAG pulsed laser at different ambient pressures was detected and analyzed. The velocities of the excited neutral Ti and Fe atoms were obtained. Under the assumption of local thermodynamic equilibrium (LTE), the electron temperature and the electron number density were deduced from, respectively, the relative line intensity and the Stark-broadening measurements conducted at different ambient pressures. Finally, the validity of application of LTE was discussed.

## 1 Experimental

A schematic diagram of the experimental arrangement is illustrated in Fig. 1. The 1.06- $\mu\text{m}$  radiation with 10-ns pulse width (full width at half maximum) produced from a Q-switched Nd:YAG laser device (Quanta Ray DCR-3) was used in the experiment. Its maximum output energy was 1 J. The laser energy was measured by a digital energy meter (Ophir DGX-30A). The laser pulse was reflected by a prism M, and was then focused onto the polished Ti alloy target surface by a quartz focusing lens L1 ( $f = 6.3$  cm). The spot size of the laser beam was 0.66 mm in diameter. The Ti alloy sample was positioned on a sample holder in a chamber pumped by a mechanical pump. The chamber and lens L1 were mounted on two two-dimensional movable plates. By adjusting synchronistically these two plates along the direction of the incident laser beam, the plasma emission spectrum was recorded as a function of the distance  $d$  from the target surface. In the direction perpendicular to the incident laser beam, two cylindrical lenses (L2 and L3) were used to image,

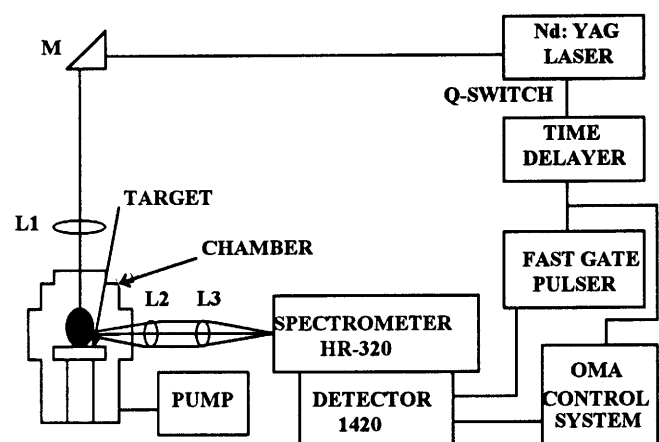


Fig. 1. Schematic diagram of the experimental arrangement

at 1:1, the plasma optical emission from the plane which has a distance  $d$  from the surface of the target, onto the entrance of the slit of an ISA(HR-320) spectrum analyzer. The dispersed emission was subsequently detected by an optical multichannel analyzer (Parc OMA III). The spectrometer of the OMA system is equipped with a 1200-grooves/mm grating, and the slit width is 25  $\mu\text{m}$ . A fast pulser (Parc model 1302) was used for gating the photodiode array, and the gate width is 10 ns. An accurate trigger delayer, which was synchronistically triggered by the electric Q-switched signal produced by the YAG laser device, was used to control the delay time at which the spectrum was recorded. Moreover, a photo diode and a digitizing oscilloscope (Tektronix TDS 620A) were used to calibrate the time delay. By changing the delay time  $t_d$ , one can get the time-resolved emission spectra.

## 2 Results and discussion

### 2.1 Plasma emission

Figure 2 shows the plasma spectra obtained at three different time delays in the wavelength range 438–450 nm at an observation distance  $d = 1.0$  mm from the target surface. The laser power density was  $3.5 \times 10^9$   $\text{W cm}^{-2}$  and the ambient pressures were (a)  $1.0 \times 10^5$  Pa and (b) 100 Pa. From Fig. 2a, it is

observed that during the initial period of the laser pulse reaching the target surface (40 ns), continuum emission is very intense. The continuum emission quickly decreases with increase of the delay time. There are also two spectral lines from  $\text{N}^+$  ions at 444.7 nm and  $\text{O}^+$  ions at 441.49 nm superposed on the continuum, but they quickly disappear because of the recombination of electrons with ions. At first, the density of ejected species is very high, and the two lines are very broad because of Stark broadening. Then, the lines become narrower. From Fig. 2b, it is observed that the signals of  $\text{N}^+$  and  $\text{O}^+$  ions are too small to be found at 100 Pa because of the reduction of atomic density of the air.

With the increase of time, isolated lines of excited Ti and Fe atoms emerge, as shown in Figs. 2a,b. Figure 3 shows the TOF curves of the Ti I 439.39 nm line from a Ti alloy sample irradiated by the pulsed laser at a flux  $3.5 \times 10^9$   $\text{W cm}^{-2}$ . The intensities of the lines were obtained by integrating the peak area with automatic spectral baseline correction. Because the concentration of the excited atoms or ions is proportional to the intensity of the spectral line, the recorded changes of the intensity of the spectral line at different time delays give information on the excited atoms or ions in the ejected vapor.

In Fig. 3, the intensities of lines obtained at an atmospheric pressure of air last for a long time, up to 8000 ns. They can last for 2000 ns at 100 Pa, (only powerful lines were retained in Fig. 3). These time intervals are much longer than

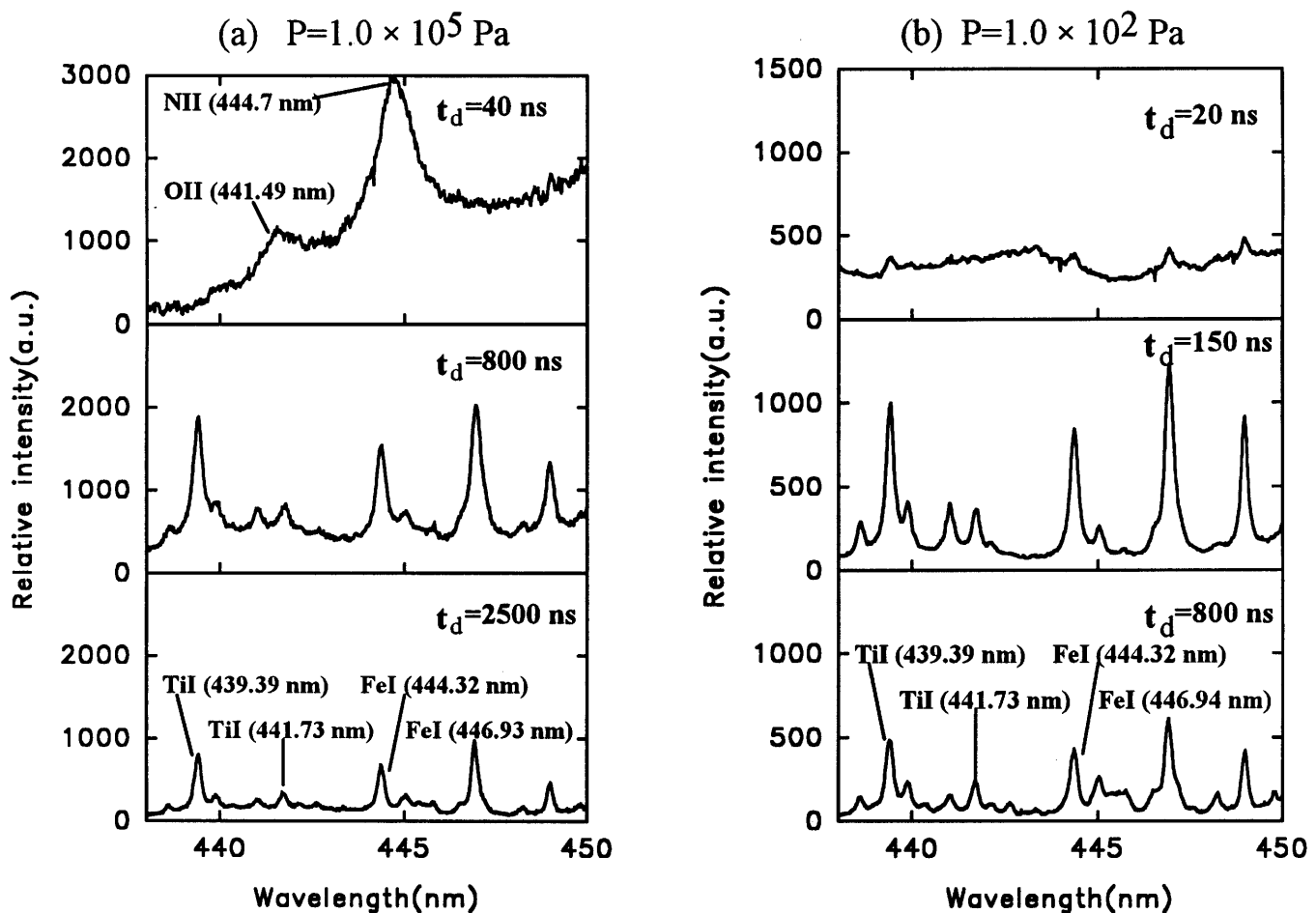


Fig. 2a,b. Evolution of plasma emission spectra in the wavelength region of 438–450 nm

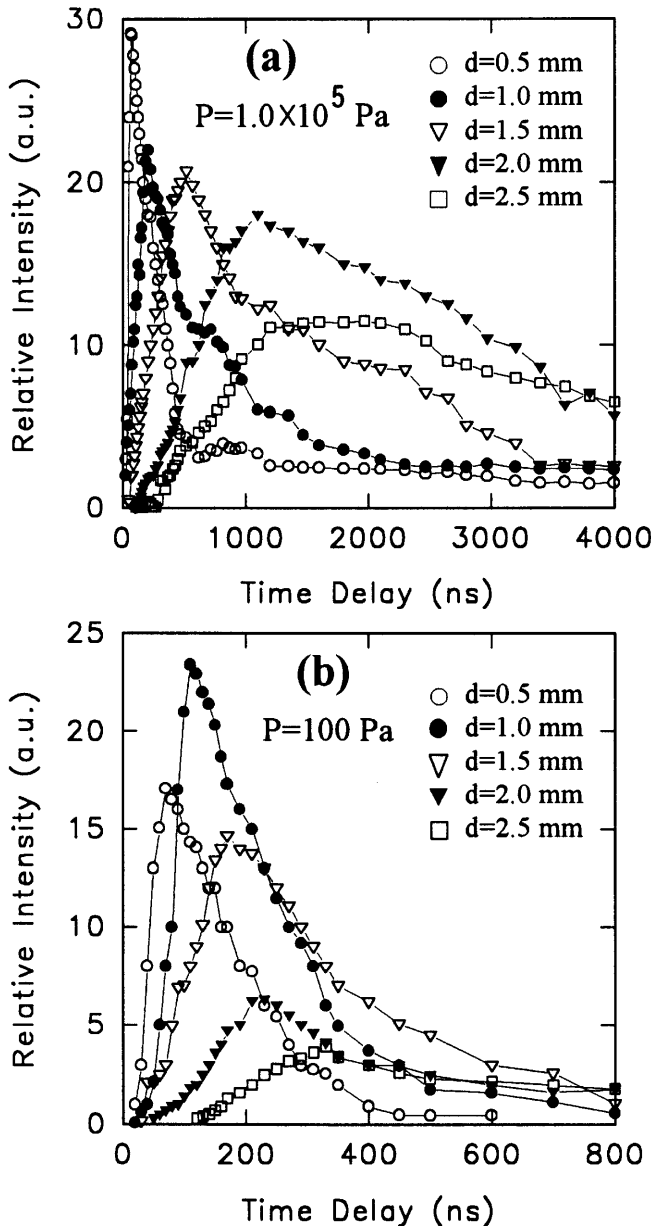


Fig. 3a,b. The TOF curves of the Ti I 439.39 nm line as obtained at different distances from the target surface

the lifetime of the excited state of Ti atom, so it can be concluded that Ti atoms are constantly produced and excited during travel to the laser source, the exciting energy comes from the plasma itself. Moreover, the lines obtained at  $1.0 \times 10^5$  Pa

pressure last for much longer than those at 100 Pa. This is because the ambient air impedes the expansion of the plasma, which would cause an increase in both emission lifetime and emission intensity. The spatial confinement of the plasma becomes stronger with increase of the ambient pressure, so the emission lifetime at  $1.0 \times 10^5$  Pa pressure is longer than that at 100 Pa.

## 2.2 Particle velocity

In Fig. 3, the emission intensity of Ti atoms is proportional to the number of excited Ti atoms. The time delays therefore embody the velocities of the atoms, so the maximum intensity for each curve as shown in Fig. 3 can be used to estimate the expansion velocity, based on the delay time [8–10]. Dividing the distance between two positions by the corresponding delay time difference gives the population-averaged velocity of the excited atoms. Table 1 lists all measured results at three different ambient pressures. The laser power density was  $3.5 \times 10^9$  W cm<sup>-2</sup>.

From Table 1, it can be found that the velocities decrease with the distance from the target surface. Moreover, the velocities of the atoms decrease with increase of the distance more rapidly at higher pressure than at lower pressures. The reason must be that increased pressure slows the velocities of the atoms by the collisions between air particles and the ejected atoms, i.e. the expansion is impeded. A similar effect occurs with the plume of particles, as distinct from individual excited state atoms, emitted when surfaces are bombarded with laser pulses [11]. Comparing the velocity of Ti atoms with that of Fe atoms, one finds that there is no great difference. We also investigated the dependence of the velocity on the laser energy. The results show that the velocity of the excited atom increases slightly with the increase of the laser energy, and this variation is more obvious at lower pressures. Similar results apply also to the plume [12].

## 2.3 Electron temperature and density

Under the assumption of LTE, the electron temperature in the plasma can be determined by relative line intensity measurements. If one observes two isolated lines, say 1 and 2, with central wavelength  $\lambda_1$  and  $\lambda_2$ , respectively, emanating from the same atomic or ionic species and if the energy level population is distributed according to the Boltzmann law, the relative intensity of these two lines,  $\varepsilon_1/\varepsilon_2$ , is given by [13]

$$\frac{\varepsilon_1}{\varepsilon_2} = \frac{g_m(1)A_{mn}(1)\lambda_2}{g_m(2)A_{mn}(2)\lambda_1} \exp\left[-\frac{E_m(1) - E_m(2)}{kT}\right], \quad (1)$$

Table 1. The average velocities of the excited atoms at different positions and pressures (m/s)

Emission line	Pressure/Pa	Position/mm			
		0.5 ~ 1.0	1.0 ~ 1.5	1.5 ~ 2.0	2.0 ~ 2.5
Ti I 439.39 nm	$1.00 \times 10^5$	$3.60 \times 10^3$	$2.00 \times 10^3$	$9.09 \times 10^2$	$6.25 \times 10^2$
	$1.00 \times 10^3$	$1.00 \times 10^4$	$8.33 \times 10^3$	$5.56 \times 10^3$	$4.00 \times 10^3$
	5.0	$1.25 \times 10^4$	$1.25 \times 10^4$	$1.00 \times 10^4$	$8.33 \times 10^3$
Fe I 446.94 nm	$1.00 \times 10^5$	$3.33 \times 10^3$	$2.25 \times 10^3$	$1.00 \times 10^3$	$5.00 \times 10^2$
	$1.00 \times 10^3$	$1.25 \times 10^4$	$9.09 \times 10^3$	$7.14 \times 10^3$	$5.56 \times 10^3$
	5.0	$1.25 \times 10^4$	$1.00 \times 10^4$	$9.09 \times 10^4$	$7.14 \times 10^3$

where  $A_{mn}(i)$  is the transition probability from energy level  $m$  to  $n$ ,  $g_m(i)$  is the statistical weight of the upper energy level,  $E_m(i)$  is the energy of the upper energy state  $m$ , and  $T$  is the electron temperature. From (1), the electron temperature can be determined provided  $A_{mn}(i)$ ,  $g_m(i)$ , and  $E_m(i)$  are known. In the present work, in order to enhance the accuracy of the measurement, five lines from excited neutral Ti atoms were chosen to determine the electron temperature. The atomic spectra data needed in (1) are listed in Table 2. These data were found from [14]. The electron temperatures obtained at two different pressures are shown in Fig. 4, the results having been acquired at 1.0 mm from the target surface. It can be found that in the early stage of plasma evolution the electron temperature is very high, and then decreases quickly with increasing time delay. Moreover, the temperature decreases with increase of time more quickly at 1000 Pa than at  $1.0 \times 10^5$  Pa, which was probably caused by the spatial confining effect of the air on the plasma. After about 300 ns at  $1.0 \times 10^5$  Pa and 200 ns at 1000 Pa, the plasma is cooled to a much lower temperature, and after there the temperature decreases very slowly.

The number density of the electrons in the plasma can be obtained from the Stark-broadening measurement of the individual lines. For singly ionized non-hydrogenic ions Stark broadening is caused predominantly by electron impact. The full width of half maximum of the lines  $\Delta\lambda_{1/2}$  is related to the

electron density  $N_e$  [13]:

$$\Delta\lambda_{1/2} = 2W (N_e/10^{16}) + 3.5A (N_e/10^{16})^{1/4} \times \left[ 1 - \frac{3}{4} N_D^{-1/3} \right] W (N_e/10^{16}). \quad (2)$$

The first term in (2) gives the contribution from electron broadening and the second term is the ion-broadening correction,  $W$  is the electron impact parameter,  $A$  is the ionic-impact broadening parameter, and  $N_D$  is the number of particles in the Debye sphere and is given by [13]:

$$N_D = 1.72 \times 10^9 \frac{T^{3/2}}{N_e^{1/2}}, \quad (3)$$

where  $T$  is in eV and  $N_e$  in  $\text{cm}^{-3}$ . Because  $W$  and  $A$  are weak functions of temperature, we can use the values of  $W$  and  $A$  for  $T = 10\,000$  K in the calculation, namely  $W = 4.04 \times 10^{-3}$  and  $A = 0.023$ , data as obtained from [15]. Using (2) and (3) and the measured Stark-broadening data of the N II 399.5 nm line at  $d = 1.0$  mm, the electron density can be calculated. The contribution by instrumental line broadening was neglected in the calculation. The results obtained at two different pressures are shown in Fig. 5. It is found that the electron temperature decreases with increasing time quickly in the early stage of the plasma evolution, and then varies more slowly with increasing time. Comparing the evolution of the electron density obtained at two different pressures, one finds that the electron density decreases with increasing time more quickly at 1000 Pa than at  $1.0 \times 10^5$  Pa.

The assumption of LTE was used in determining the electron temperature and density. In fact a necessary (but insufficient) condition for LTE is [16]:

$$N_e \geq 1.4 \times 10^{14} T^{1/2} (E_m - E_n)^3 \text{ cm}^{-3}, \quad (4)$$

where  $T$  is the temperature in eV,  $E_m - E_n$  is the energy difference between the upper and lower states in eV.

**Table 2.** Spectroscopic data of neutral Ti lines

$\lambda_{mn}/\text{nm}$	$E_m/\text{cm}^{-1}$	$g_m$	$A_{mn}/10^8 \text{ s}^{-1}$
402.46	25227	7	0.063
439.39	41040	11	0.33
441.73	37852	9	0.36
500.72	26564	7	0.48
521.04	19574	9	0.034

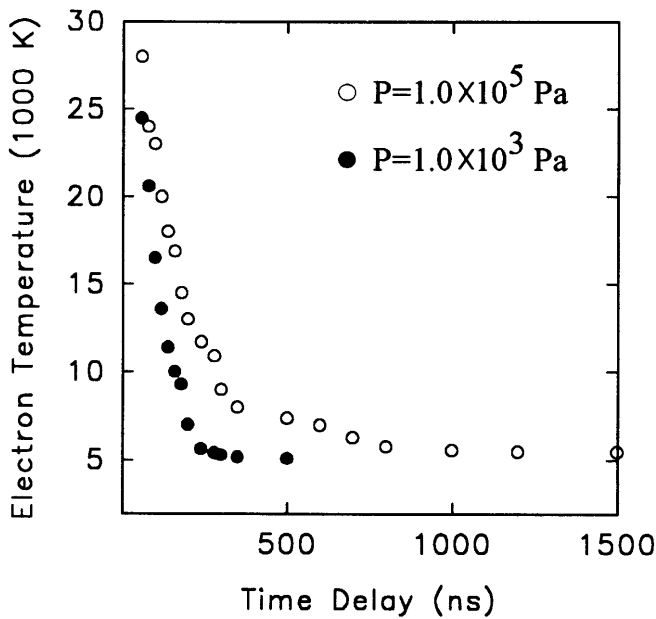


**Fig. 4.** The electron temperature of the plasma as obtained at  $d = 1.0$  mm from the target surface

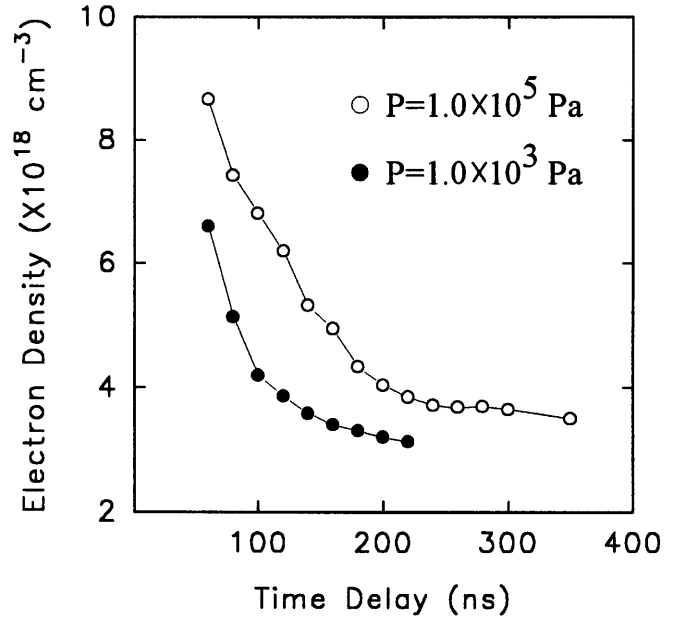


**Fig. 5.** The electron density  $N_e$  of the plasma as obtained at  $d = 1.0$  mm from the target surface

In the present work, the largest energy level difference is about 3.1 eV. The highest temperature is  $kT = 2.6$  eV. Using these values in (4), we obtained a lower limit for  $N_e$  of  $6.1 \times 10^{15} \text{ cm}^{-3}$ , which is much lower than the experimental value of  $N_e$  obtained from the Stark broadening. Therefore, it seems that the LTE assumption used in the evaluation of  $N_e$  and  $T$  in the early stage of the plasma evolution is valid.

### 3 Conclusion

The spectroscopic diagnostic method has been used to study the space- and time-resolved behavior of the pulsed laser-produced plasma from a Ti alloy target at different ambient pressures. The results show that the expansion velocities of the plasma, the electron temperature, and the electron density are all influenced by the ambient pressure. The velocity of the excited atom decreases with increase of the distance from the target surface more slowly at lower pressure. However, the electron temperature and density decrease with increase of the time delay more quickly at lower pressure. The effects on these properties of the plasma are very important for understanding the mechanisms of laser-materials interaction as well as for quality control in preparing thin films by using the PLD technique.

### References

1. H. Wang, A.P. Salzberg, B.R. Weiner: *Appl. Phys. Lett.* **59**, 935 (1991)
2. H. Izumi, K. Ohata, T. Sawada, T. Morishita, S. Tanaka: *Appl. Phys. Lett.* **59**, 597 (1991)
3. H. Tabata, T. Kawai: *Thin Solid Films* **225**, 275 (1993)
4. H.P. Gu, Q.H. Lou, N.H. Cheung, S.C. Chen, Z.Y. Wang, P.K. Lin: *Appl. Phys. B* **58**, 143 (1994)
5. M. Kuzuya, H. Matsumoto, H. Takechi, O. Mikami: *Appl. Spectrosc.* **47**, 1659 (1993)
6. Y. Iida: *Spectrochim. Acta B* **45**, 1353 (1990)
7. Y.I. Lee, T.L. Thiem, G.H. Kim, Y.Y. Teng, J. Sneddon: *Appl. Spectrosc.* **46**, 1597 (1992)
8. P.J. Wolf: *J. Appl. Phys.* **72**, 1280 (1992)
9. A.D. Sappy, T.K. Gamble: *Appl. Phys. B* **53**, 353 (1991)
10. C. Girault, D. Damiani, J. Aubreton, A. Catherinot: *Appl. Phys. Lett.* **55**, 182 (1989)
11. R. Kelly, A. Miotello: *Nucl. Instrum. Methods B* **122**, 374 (1997)
12. A. Giardini Guidoni, R. Kelly, A. Mele, A. Miotello: *Plasma Sources Sci. Technol.* **6**, 260 (1997)
13. G. Bekefi: *Principles of Laser Plasmas*, ed. by G. Bekefi (Wiley, New York 1976) p. 593
14. W.L. Wiese, M.W. Smith, B.M. Miles: *Atomic Transition Probabilities* (National Stand. Ref. Data Ser., Washington DC 1969) p. E-365
15. H.R. Griem: *Plasma Spectroscopy* (Mc Graw-Hill, New York 1964) p. 463
16. R.W.P. McWhirter: *Plasma Diagnostic Techniques*, ed. by R.H. Huddleston, S.L. Leonard (Academic Press, New York 1965) p. 206